Journal of Nuclear Materials 384 (2009) 56–60

Contents lists available at ScienceDirect

Journal of Nuclear Materials

journal homepage: www.elsevier.com/locate/jnucmat

The effect of alloying elements on the vacancy defect evolution in electron-irradiated austenitic Fe–Ni alloys studied by positron annihilation

A.P. Druzhkov *, D.A. Perminov, A.E. Davletshin

Institute of Metal Physics, Ural Branch RAS, 18 Kovalevskaya St., 620041 Ekaterinburg, Russia

ARTICLE INFO

Article history:
Received 6 June 2008
Accepted 20 October 2008

PACS:
61.72.Ji
61.82.Bg
78.70.Bj

ABSTRACT

The vacancy defect evolution under electron irradiation in austenitic Fe–34.2 wt% Ni alloys containing oversized (aluminum) and undersized (silicon) alloying elements was investigated by positron annihilation spectroscopy at temperatures between 300 and 573 K. It is found that the accumulation of vacancy defects is considerably suppressed in the silicon-doped alloy. This effect is observed at all the irradiation temperatures. The obtained results provide evidence that the silicon-doped alloy forms stable low-mobility clusters involving several Si and interstitial atoms, which are centers of the enhanced recombination of migrating vacancies. The clusters of Si-interstitial atoms also modify the annealing of vacancy defects in the Fe–Ni–Si alloy. The interaction between small vacancy agglomerates and solute Al atoms is observed in the Fe–Ni–Al alloy under irradiation at 300–423 K.

1. Introduction

Understanding the role of alloying elements on the defect structural evolution is important for the development of reactor materials. It is known [1] that alloying elements in alloys and steels have a considerable effect on microstructural and microchemical evolution under irradiation. The consideration usually is given to the role of alloying atoms in both the solid solution and precipitates of secondary phases. The size factor has the decisive effect on the character of the interaction between alloying atoms and point defects in the solid solution. In nickel and austenitic Fe–Cr–Ni and Fe–Ni alloys, undersized impurity atoms (P, Si) interact predominantly with interstitial atoms [2–5], while oversized impurities (Ti, Nb) interact with vacancies [3,6,7]. The formation of stable low-mobility complexes of interstitial atoms or vacancies with impurity atoms increases the recombination of point defects and, hence, changes the formation kinetics of defect clusters. These processes can present a significant factor for the kinetics of such phenomena as the radiation-induced segregation, creep and void swelling.

Our previous studies [8–10] demonstrated the effect of nano-sized intermetallic precipitates (like Ni_3Al) on the evolution of vacancy defects in a Fe–Ni–Al model alloy. This study deals with the effect of alloying elements in the solid solution. We analyzed the accumulation and the subsequent annealing of vacancy clusters in austenitic Fe–Ni alloys doped with silicon and aluminum (3–6 wt% or 6–11 at.%). Aluminum and silicon atoms are oversized and undersized atoms in this alloy, respectively [11]. On the basis of size factor, a strong 'interstitial atom (IA)–solute' interaction is expected for the Si solute, but not for Al [12]. Austenitic Fe–Ni–Al(Si) alloys served as model alloys of fast breeder reactor stainless steels. Point defects were induced by electron (5 MeV) irradiation at 300–573 K, generating homogeneously distributed Frenkel pairs. Defects were diagnosed using the positron annihilation spectroscopy (PAS) whose physical principles are described comprehensively in [13,14]. It is well-known that positrons are a sensitive probe of vacancy defects, with sensitivity starting from the atomic size to large vacancy clusters or nanovoids [15].

2. Materials and methods

Fcc Fe–Ni–Al (34.2 wt% Ni, 5.4 wt% Al, C $\leqslant$ 0.01 wt%, the balance Fe), Fe–Ni–Si (34.2 wt% Ni, 2.9 wt% Si, C $\leqslant$ 0.01 wt%, the balance Fe) and Fe–Ni (36.5 wt% Ni) alloys were used. After rolling, cutting and electrochemical polishing, samples about $10 \times 10\ mm^2$ in size (0.2–0.3 mm thick) were annealed under a 10^{-6} Pa vacuum at 1373 K for 1 h and quenched in water at room temperature. The presence of one austenitic phase in the samples was checked by the X-ray analysis. The microstructure of the solution-annealed samples was certified using a JEM-200 CX electron microscope at an accelerating voltage of 160 kV. Samples had grains ~50 μm in size and the dislocation density of about $10^{11}\ m^{-2}$.

Samples of the Fe–Ni–Al(Si) and Fe–Ni alloys were irradiated at 300–573 K with 5 MeV electrons in a linear accelerator. The samples were positioned as tightly as possible in the center of the irradiation zone ($10 \times 10\ mm^2$) of the sample holder and the electron beam sweeping was applied to provide homogeneous irradiation.

* Corresponding author. Tel.: +7 343 378 38 62; fax: +7 343 374 52 44.
E-mail address: druzhkov@imp.uran.ru (A.P. Druzhkov).

0022-3115/$ - see front matter © 2008 Elsevier B.V. All rights reserved.
doi:10.1016/j.jnucmat.2008.10.002

After irradiation to half of the total fluence, the sample holder with the specimens was reversed in order to obtain a symmetric distribution of damage in the samples. The irradiation temperature was controlled to within ±5 K. The maximum electron fluence was 5×10^{22} m^{-2}. The fluence concerned with damaging dose by:

$$D(E_e) = \phi \sigma^e_{eff}(E_e), \quad (1)$$

where E_e is the electron energy, ϕ *is the* electron fluence, σ^e_{eff} is the effective cross-section for displacement of atoms by an electron calculated by the modified Kinchin–Pease model [16]. The maximum fluence corresponds to the damaging dose of $\sim 5 \times 10^{-4}$ dpa irrespectively of the alloying elements.

The irradiated samples were isochronally annealed (stepwise, 25–50 K per step) in a vacuum over the temperature interval from 300 to 850 K at an average heating rate of 1 K min^{-1}.

Positron states in vacancy-type defects were diagnosed by angular correlation of annihilation radiation (ACAR), which is one of positron annihilation techniques [13,14]. ACAR method was realized in a one-dimensional ACAR spectrometer providing a resolution of 1 mrad × 160 mrad [10]. A ^{68}Ge positron source of activity of 350 MBq was used. At least 6×10^5 coincidence counts were collected in each ACAR spectrum; the peak-to-background ratio was $\sim 10^3$. The ACAR spectra represented the dependence of the coincidence count rate on the angle θ (θ being the deviation of annihilation γ-quanta from anticollinearity). The angle $\theta = p_z/m_0c$, where p_z is the transverse component of the momentum of an electron–positron pair, m_0 is the rest mass of an electron, and c is the light velocity.

Changes in the shape of the ACAR spectra were characterized by the standard S-parameter [10]. The S-parameter was defined as the ratio of the sum of the coincidence count rate at θ from 0 to 3.5 mrad to the full coincidence count rate. The S-parameter characterized the probability of annihilation of positrons with nearly free electrons. When positrons were trapped at vacancy defects, the S-parameter increased [10].

According to the simple trapping model (STM) [17], the S-parameter is related to the concentration of defects (e.g., small vacancy clusters) C_{cl} as;

$$C_{cl} = \frac{\lambda_f (S - S_f)}{\mu_{cl}(S_{cl} - S)}, \quad (2)$$

where λ_f is the positron annihilation rate in the bulk (free) state; μ_{cl} is the specific positron trapping rate; S_f and S_{cl} are the S-parameters characteristic of the positron annihilation from the bulk (free) and defect-trapped states, respectively. In the case of small three-dimensional vacancy clusters (VCs), $\mu_{cl} \approx n\mu_v$ [18] (n being the cluster multiplicity and μ_v the specific trapping rate for monovacancies). The STM is correctly applicable to homogeneously distributed defects in materials (e.g., in the case of electron irradiation).

3. Results

3.1. Accumulation of vacancy defects

Figs. 1–3 present the dependence of the S-parameter on the electron fluence for Fe–Ni–Al and Fe–Ni–Si alloys exposed to irradiation at 300, 423 and 573 K, respectively. The data for the Fe–Ni–Al alloy are taken from our previous work [8]. In [8] the quenched state of the Fe–Ni–Al alloy is designated as the Q-state. For comparison, Figs. 2 and 3 show $S(\phi)$ for the binary Fe–Ni alloy [7]. In the initial state (before irradiation) the S-parameter is larger in samples of the Fe–Ni–Al alloy. This is because the concentration of aluminum in the solid solution of the alloy is higher than that of silicon. In the unirradiated samples positrons annihilate from

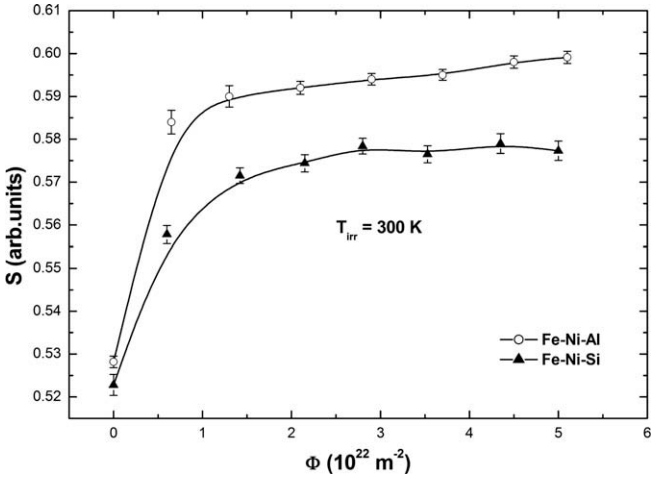

Fig. 1. Variation of the S-parameter as a function of the electron fluence for the Fe–Ni–Al and Fe–Ni–Si alloys irradiated at 300 K. The data for the Fe–Ni–Al alloy are taken from a previous study [8].

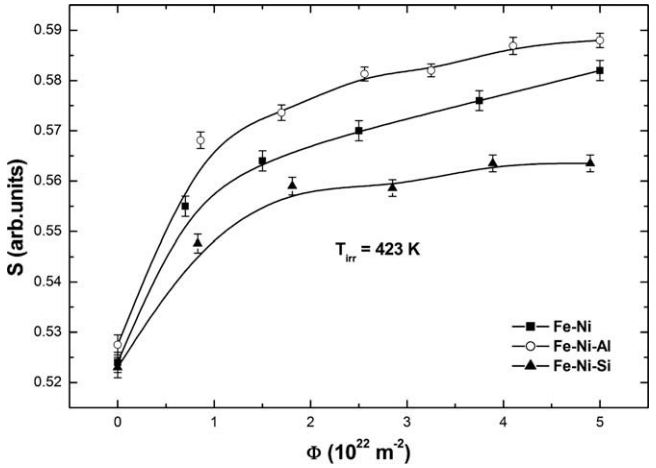

Fig. 2. Variation of the S-parameter as a function of the electron fluence for the Fe–Ni, Fe–Ni–Al and Fe–Ni–Si alloys irradiated at 423 K. The data for the Fe–Ni and Fe–Ni–Al alloys are taken from previous studies [7,8], respectively.

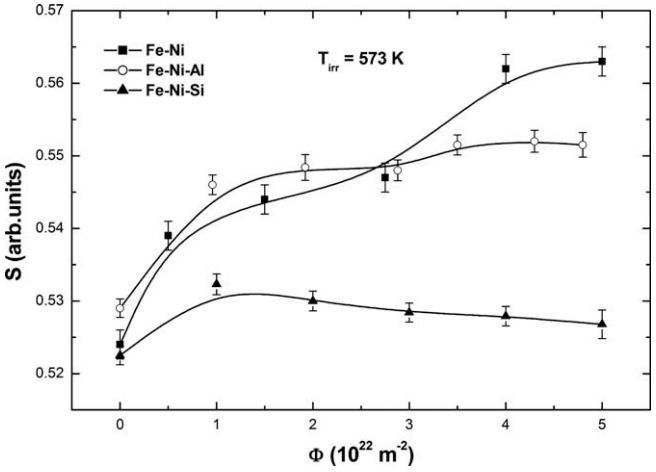

Fig. 3. Variation of the S-parameter as a function of the electron fluence for the Fe–Ni, Fe–Ni–Al and Fe–Ni–Si alloys irradiated at 573 K. The data for the Fe–Ni and Fe–Ni–Al alloys are taken from our previous studies [7,8], respectively.

free states, because the concentration of quenched vacancies in austenitic alloys usually is lower than the PAS sensitivity limit [19] since the thermal conductivity of these alloys is low.

As the fluence increases, the S-parameter grows whatever the alloy.

Let us consider first the behavior of the S-parameter in samples of the Fe–Ni–Al alloy. Whatever the irradiation temperature, the dependence $S(\phi)$ exhibits the following trend: (a) the S-parameter increases considerably as the fluence rises to $(1.5-2.0)\times 10^{22}\ m^{-2}$; (b) the S-parameter increases insignificantly at higher fluencies. Thus, a quasi-steady state [20] is established at a fluence larger than $2.0\times 10^{22}\ m^{-2}$. It was demonstrated earlier [5] that vacancies are mobile at room temperature in fcc Fe–Ni alloys of the invar composition. The increment of the S-parameter at the irradiation temperature of 300 K is due to the trapping of positrons at small three-dimensional VCs. The concentration and the structure of VCs change little in the quasi-steady state.

As the temperature is elevated, interstitial atoms and vacancies become more mobile and, correspondingly, the probability of both the mutual recombination of point defects and their absorption on sinks increases [20]. As a result, the concentration of accumulated VCs drops and the S-parameter acquires smaller values with growing irradiation temperature (see Figs. 1–3). It should be noted also that the configuration of VCs changes too as the irradiation temperature rises. For example, if the irradiation temperature is 573 K, the prevailing clusters are two-dimensional VCs, e.g., small vacancy loops [5], for which the S-parameter is smaller than its counterpart for three-dimensional VCs.

The behavior of the dependence $S(\phi)$ for the Fe–Ni–Si alloy is similar to the behavior of the S-parameter in the Fe–Ni and Fe–Ni–Al alloys. However, plateaus of the S-parameter are much lower and this effect is enhanced with the irradiation temperature. If the irradiation temperature is 573 K, the value of the S-parameter changes little with the fluence (see Fig. 3). Thus, silicon as the alloying element in the Fe–Ni matrix considerably limits the increments of the S-parameter under irradiation as compared to aluminum.

3.2. Annealing of vacancy defects

Fig. 4 presents the S-parameter versus the isochronal annealing temperature of the Fe–Ni–Al and Fe–Ni–Si alloys exposed to a fluence of up to $5\times 10^{22}\ m^{-2}$. The data for the Fe–Ni–Al alloy are taken from [8].

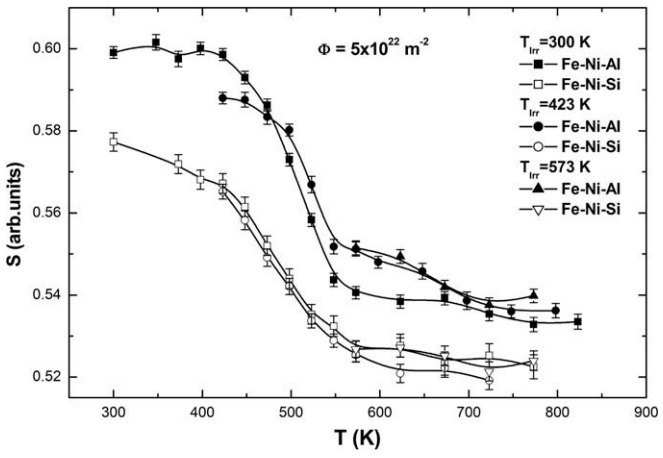

Fig. 4. Evolution of the S-parameter as a function of the isochronal annealing temperature in irradiated Fe–Ni–Al and Fe–Ni–Si alloys at 300, 423 and 573 K, respectively. The data for the Fe–Ni–Al alloy are taken from a previous work [8].

Let us analyze the behavior of the S-parameter during annealing of the Fe–Ni–Al alloy. The S-parameter begins decreasing quickly at annealing temperatures above 420 K and the decrease nearly stops by 600 K in the sample, which was irradiated at room temperature. The quick drop of the S-parameter is due to the dissociation of VCs. The S-parameter of the sample irradiated at 423 K begins decreasing nearly at the same annealing temperatures, but the drop of the S-parameter decelerates at temperatures above 550 K. The slow drop of the S-parameter at temperatures from 550 to 750 K is connected with annealing of thermally more stable two-dimensional configurations of vacancy clusters, which appeared either during irradiation at 423 K or during annealing as a result of the conversion of three-dimensional configurations of VCs to their two-dimensional configurations. Indeed, the S-parameter of the sample irradiated at 573 K behaves itself analogously to the S-parameter at the high-temperature stage of recovery in the sample irradiated at 423 K (see Fig. 4). It was mentioned in Section 3.1 that small vacancy loops are formed mainly under irradiation at 573 K. It should be noted that the S-parameter does not recover its initial values (before irradiation) for the samples, which were irradiated at 300, 423 K and annealed at ~800 K. Unfortunately, the further increase in the annealing temperature leads to thermal aging of the alloy and the localization of positrons in nanosized particles of Ni_3Al [8]. Note also the growth of the S-parameter in the sample, which was irradiated at 573 K and annealed at 773 K (see Fig. 4). The S-parameter increases due to 'trapping' of positrons by intermetallic particles, which are formed owing to radiation-induced aging (see [8]).

As distinct from the Fe–Ni–Al alloy, the S-parameter in the Fe–Ni–Si alloy begins decreasing slowly at annealing temperatures above 300 K. The largest drop of the S-parameter is observed over the same temperature interval as in the Fe–Ni–Al alloy. A characteristic feature of the annealing of vacancy defects in Fe–Ni–Si is that the dependence $S(T_{ann})$ after irradiation at 423 K nearly coincides with $S(T_{ann})$ after irradiation at 300 K. The high-temperature (above 580 K) stage, which is connected with annealing of vacancy loops, is considerably suppressed as compared to the corresponding stage in the Fe–Ni–Al alloy. Thus, one annealing stage dominates in the silicon-doped alloy irrespectively of the irradiation temperature.

4. Discussion

4.1. Effect of aluminum

The above results demonstrate that alloying elements have a considerable effect on the evolution of vacancy defects in the fcc Fe–Ni model alloy. Being an oversized impurity, aluminum can interact with vacancies. This interaction modifies the process of the accumulation of vacancy defects and their thermal stability. It was shown in our recent paper [7] that doping of the Fe–Ni alloy with titanium leads to the accumulation of an enhanced concentration of fine VCs under irradiation at 270–423 K. It is known [21] that impurities, which strongly interact with vacancies, represent nucleation centers of vacancy clusters. When the concentration of the nuclei is high (suitable impurities), VCs are larger in number and smaller in size. As a result, the values of the S-parameter are higher than those in the undoped Fe–Ni alloy (see [7]). This situation is also characteristic of the Fe–Ni–Al alloy irradiated at 423 K. The S-parameter reaches higher values as compared to those in the undoped Fe–Ni alloy (see Fig. 2). The annealing of vacancy clusters in the aluminum-doped alloy irradiated at 300 and 423 K begins approximately at the same temperatures as in the undoped alloy (see Fig. 4 and [7]). This fact suggests that in the Fe–Ni alloy the binding energy between vacancies and Al atoms is lower than that

between vacancies and Ti atoms. Indeed, the Al-vacancy binding energy in nickel is estimated at 0.05–0.08 eV [1,21].

As the irradiation temperature increases, the vacancy–impurity interaction becomes less efficient. The effect of the alloying element can show up through other mechanisms. The Fe–Ni–Al alloy is a supersaturated solid solution and it decomposes during the thermal or radiation-induced aging. This is followed by the precipitation of nanosized particles of the γ'-phase. We showed earlier [8–10] that these particles retard the accumulation of vacancy defects. For example, at 573 K the accumulation of vacancy defects in the Al-doped alloy is suppressed as compared to their accumulation in the Fe–Ni binary alloy (see Fig. 3). This is due to the radiation-induced formation of fine intermetallic particles like Ni_3Al [8].

4.2. Effect of silicon

It was shown earlier [2,3] that silicon atoms interact strongly with interstitial atoms and weakly with vacancies in austenitic alloys and nickel. The interaction of silicon atoms with interstitial atoms has a considerable effect on the accumulation of vacancy defects under electron irradiation at temperatures of 300–573 K. As Si is an undersized element in Fe–Ni, interstitials will easily be trapped by silicon [12]. With increasing fluence, a large amount of trapped interstitial atoms (Si-IA) and their clusters will be formed. They work as an effective site for the recombination of freely migrating vacancies and suppress the growth of the number and (or) the size of vacancy clusters. The vacancy path length to a recombination center is the shortest in this case and, therefore, the vacancy clustering is the least. For this reason the values of the S-parameter in the quasi-stationary state are smaller in the Fe–Ni–Si alloy than they are in the Fe–Ni–Al and Fe–Ni alloys. Let us estimate the accumulation of vacancy defects in the Fe–Ni–Al and Fe–Ni–Si alloys at different irradiation temperatures.

4.2.1. Irradiation at 300 K

According to the STM estimates (Eq. (2)), the concentration of vacancies in VCs in the Fe–Ni–Si alloy is 6.5 times smaller than it is in the Fe–Ni–Al alloy (at the fluence of 5×10^{22} m^{-2}). The annihilation rate in the alloys was determined by a linear interpolation of τ_f^{-1} values of the constituent pure metals Fe, Ni, Al [22] and Si [23]. It was equal to 9.1×10^9 s^{-1} in both alloys. The μ_v value was taken equal to 2.2×10^{15} s^{-1} for pure Ni [24] as a typical value for fcc materials [19]. The S_{cl} value was 0.605 [25].

4.2.2. Irradiation at 423 K

In this case, the STM estimates show that the concentration of accumulated vacancies in the Fe–Ni–Si alloy is four times smaller than it is in the Fe–Ni–Al alloy (given the same fluence of 5×10^{22} m^{-2}). At this irradiation temperature the ratio of the accumulated vacancies in the Fe–Ni–Al and Fe–Ni–Si alloys decreased with respect to the ratio obtained at room temperature. The question arises as to the stability and/or the mobility of Si-IA clusters. These clusters will be effective recombination centers only if they are less mobile than vacancies. It is shown [2] that in the Ni–1 at.% Si alloy the clusters are less mobile as compared to the vacancies at least up to the temperatures of the annealing stage III (350–500 K). The authors state that in concentrated alloys with a high silicon concentration (>1 at.%) and at elevated irradiation temperatures the stability and a low-mobility of Si-IA clusters will be achieved due to the increase in the number of both silicon atoms and IA in the clusters. It was assumed [2] that this situation is most characteristic of neutron-irradiated alloys where the Si-IA clustering in energy displacement cascades is expected. Indeed, it was found [26] that the formation of nanovoids is retarded in neutron-irradiated Ni–2 at.% Si at 573 K. The suppression of nanovoids in this alloy is discussed from the standpoint of the Si-IA interaction. However, the results presented herein demonstrate that low-mobility Si-IA clusters are formed under electron irradiation too, producing isolated Frenkel pair defects only and do not created cascades.

4.2.3. Irradiation at 573 K

The accumulation of vacancy defects is almost completely suppressed at this temperature in the Fe–Ni–Si alloy. Thus, the Si-IA clusters, which are formed at 573 K, are stable and low-mobile and serve as effective centers of an enhanced recombination of migrating vacancies.

The accumulation of vacancy defects can be retarded by fine intermetallic particles in addition to Si-IA clusters. Similarly to the Al-doped alloy, the radiation-induced formation of precipitates like Ni_3Si is possible in the Fe–Ni–Si alloy. For example, N_3Si precipitates were detected in the Ni–4 at.% Si alloy under similar conditions of electron irradiation [27]. These precipitates can retard the accumulation of vacancy defects by analogy with Ni_3Al particles [10]. However, the assumption as to the role of nanosized Ni_3Si particles as centers of an enhanced recombination of point defects should be verified in experiments.

Si-IA clusters also have a considerable effect on the character of annealing of vacancy defects in the Fe–Ni–Si alloy. Whatever the irradiation temperature, one stage of annealing at temperatures of 400–600 K dominates. It is connected with the recombination of vacancies, which are released during the dissociation of VCs, on Si-interstitial atoms clusters. Unlike in the Fe–Ni–Al alloy, the transformation of VCs to vacancy loops at annealing temperatures above 550 K is almost completely suppressed (see Fig. 4).

Thus, our results provide evidence that a large population of stable low-mobility Si-IA clusters is formed in the Fe–Ni–Si alloy under electron irradiation at temperatures of 300–573 K, which are vacancy recombination centers.

5. Conclusions

PAS was employed to study vacancy defects evolution in Fe–Ni–Al and Fe–Ni–Si alloys. Fe–34.2 wt% Ni alloys containing 5.4 wt% Al and 2.9 wt% Si were electron irradiated at 300–573 K and subsequently isochronally annealed. The main results are summarized as follows.

(1) It was found prior to annealing that the accumulation of vacancy defects is considerably suppressed in the silicon-doped alloy at all the irradiation temperatures. These results clearly indicate that the silicon-doped alloy forms stable low-mobility Si-IA clusters, which are centers of an enhanced recombination of migrating vacancies.
(2) Si-IA clusters also influence the character of vacancy defect annealing in the Fe–Ni–Si alloy. Whatever the irradiation temperature, one stage of annealing at temperatures of 400–600 K dominates. It is connected with the recombination of vacancies, which are released during the dissociation of VCs, on Si-interstitial clusters.
(3) The interaction of vacancies with Al solute atoms in the Fe–Ni–Al alloy under irradiation at 300–423 K leads to the formation of an enhanced concentration of fine vacancy clusters, which is higher than the corresponding concentration in the Fe–Ni binary alloy.

Acknowledgements

The authors wish to thank Dr N.L. Pecherkina for her assistance in characterization of the microstructure of the initial

solution-annealed samples. The work was done with support of the Project ISTC 3074.2, RAS Program No. 01.2.00613394, RFBR (Project Nos. 07-02-00020 and 07-02-96052).

References

[1] P.R. Okamoto, L.E. Rehn, J. Nucl. Mater. 83 (1979) 2.
[2] R.S. Averback, P. Ehrhart, J. Phys. F: Met. Phys. 14 (1984) 1347.
[3] C. Dimitrov, O. Dimitrov, J. Phys. F: Met. Phys. 14 (1984) 793.
[4] H. Watanabe, H. Aoki, T. Muroga, N. Yoshida, J. Nucl. Mater. 179–181 (1991) 529.
[5] V.L. Arbuzov, A.P. Druzhkov, S.E. Danilov, J. Nucl. Mater. 295 (2001) 273.
[6] H. Watanabe, T. Muroga, N. Yoshida, J. Nucl. Mater. 239 (1996) 95.
[7] A.P. Druzhkov, V.L. Arbuzov, D.A. Perminov, J. Nucl. Mater. 341 (2005) 153.
[8] A.P. Druzhkov, D.A. Perminov, V.L. Arbuzov, J. Phys.: Condens. Matter 18 (2006) 365.
[9] A.P. Druzhkov, D.A. Perminov, Characterization of nanostructural features in reactor materials using positron annihilation spectroscopy, in: Joel E. Keister (Ed.), Nuclear Materials Research Developments, Nova Publishing Inc., New York, 2007, p. 215.
[10] A.P. Druzhkov, D.A. Perminov, N.L. Pecherkina, Phil. Mag. 88 (2008) 959.
[11] V.V. Sagaradze, V.A. Shabashov, T.M. Lapina, N.L. Pecherkina, V.P. Pilyugin, Fiz. Met. Metalloved. 78 (1994) 49;
V.V. Sagaradze, V.A. Shabashov, T.M. Lapina, N.L. Pecherkina, V.P. Pilyugin, Engl. Transl. Rus. Phys. Metals Metallogr. 78 (1994) 619.
[12] P.H. Dederichs, C. Lehmann, H. Schober, A. Scholz, R. Zeller, J. Nucl. Mater. 69&70 (1978) 176.
[13] P. Hautojarvi (Ed.), Positron in Solids, Springer, Berlin, 1979.
[14] A. Dupasquier, A.P. Mills (Eds.), Positron Spectroscopy of Solids, North-Holland, Amsterdam, 1994.
[15] M. Eldrup, B.N. Singh, J. Nucl. Mater. 251 (1997) 132.
[16] J. Morillo, C.H. de Novion, J. Dural, Radiat. Eff. 55 (1981) 67.
[17] W. Brandt, Appl. Phys. 5 (1974) 1.
[18] R.M. Nieminen, J. Laakonen, Appl. Phys. 20 (1979) 181.
[19] U. Holzwarth, A. Barbieri, S. Hansen-Ilzhofer, P. Schaaff, M. Haaks, Appl. Phys. A 73 (2001) 467.
[20] A.C. Damask, G.J. Dines, Point Defects in Metals, Gordon and Breach, London, 1963.
[21] G. Dlubek, R. Krause, O. Brummer, Z. Michno, T. Gorecki, J. Phys. F: Met. Phys. 17 (1987) 1333.
[22] R. Wurschum, K. Badura-Gergen, E.A. Kummerle, C. Grupp, H.-E. Schaefer, Phys. Rev. B 54 (1996) 849.
[23] M.J. Puska, R.M. Nieminen, Rev. Mod. Phys. 66 (1994) 841.
[24] G. Dlubek, O. Brummer, E. Hensel, Phys. Stat. Sol. (a) 34 (1976) 737.
[25] A.P. Druzhkov, V.L. Arbuzov, D.A. Perminov, Fiz. Met. Metalloved. 94 (2002) 75;
A.P. Druzhkov, V.L. Arbuzov, D.A. Perminov, Engl. Transl. Rus. Phys. Metals Metallogr. 94 (2002) 68.
[26] T. Yoshiie, Q. Xu, Y. Satoh, H. Ohkubo, M. Kiritani, J. Nucl. Mater. 283–287 (2000) 229.
[27] A. Barbu, G. Martin, A. Chamberod, J. Appl. Phys. 51 (1980) 6192.